Triazine-based porous organic polymer for selective oxidation of α-aryl substituted olefins cleavage into benzaldehydes

4.1 Abstract

This chapter describes the synthesis of a new triazine ring based porous organic polymer. This polymer is employed as organocatalyst in aryl olefins oxidation into benzaldehyde. A metal free, high nitrogen content and π-electrons rich organic polymer acting as a catalyst in the unusual Wacker-Type oxidation of olefins into benzaldehyde selectively is a rare outcome. The role of such porous polymer as catalyst has further tested successfully to cleave carbon-carbon triple bonds. Results are supported by experimental findings. The reaction mechanism is proposed based on computational investigations. Thus present study emphasizes potent application of nitrogen rich POPs as heterogeneous organic catalyst in performing organic reactions with no metal adds-on.

4.2 Introduction

Wacker-type oxidation of olefins to the corresponding ketone and/or aldehyde is important from synthetic organic chemistry perspective. But, selective oxidation into desired carbonyl product, especially the aldehyde is a challenge. Use of precious metal catalyst (Pd, Ru etc.) and other metals such as Ni, Cu, Co, or mixed metals, etc. were found effective towards Wacker-type oxidations but with compromised selectivity and percentage product yield [1-3]. To note, Wacker-type oxidation is generally accomplished by transition metal catalyst producing methyl ketone as the primary product following Markovnikov's rule producing aldehyde in little to nil quantity [4-6]. With aryl alkenes such as styrene the regiospecificity is altered yielding aldehyde as the major product following *anti*-Markovnikov's rule [7-9]. The majority studies disclose the formation of methyl ketone selectivity following Markovnikov's rule. Such oxidation is accomplished by the presence of peroxometal species using molecular oxygen or peroxides as the oxidant. Sigman and co-workers demonstrated the involvement of peroxide as anion while explaining the mechanism of palladium catalyzed alkene oxidation using quinoline-2-oxazoline ligand [10]. Similar mechanistic pathway with Pd-hydroperoxide intermediate has also been discussed by Muldoon and his group [4]. The

formation of methyl ketone selectivity in terminal olefins oxidation is customary following Markovnikov's rule.

Literature review evidences the advancement in selective oxidation of terminal olefins into aldehydes [7,8,11]. But selective oxidation with *anti*-Markovnikov's product formation is not obvious [12]. The common synthetic route of such oxidation is accomplished by the presence of catalytic nitrite along with other metal catalyst. For example, the styrene oxidation is restricted to 2-phenyl acetaldehyde formation. Perhaps epoxidation of olefin in metal catalyzed oxidation can easily be perceived and well documented [13]. Thus the formation of benzaldehyde via C=C double bond cleavage with high selectivity is extremely rare though such cleavage with poor selectivity has been accomplished in presence of transition metal catalysts [14,15]. A water soluble Pd(II) complex was explored as an efficient catalyst in the selective oxidation of styrene [15]. It witnesses the formation of benzaldehyde by the cleavage of terminal C=C double bond of styrene. The fastest oxidation of styrene yielding benzaldehyde has been reported using C-scorpionate Cu(II) complex as heterogeneous catalyst [16]. A copper docked imine linked 2D covalent organic framework (COF) having π-stacked highly ordered structure with increased crystallinity has been recently developed to promote catalytic oxidation of styrene to afford benzaldehyde [17].

Applications of POP as heterogeneous catalyst with or without metal incorporation in performing various organic transformation reactions are documented and a recent trend [18-20]. Most of the reported POPs discloses the linking of building units via imine linkages in wide and few having the triazine connectivity. In this context, introducing appropriate and tuned functionalities into POPs with π-conjugated skeleton envisage potential applications in heterogeneous catalysis, in gas adsorption, etc. Bhaumik et al. recently synthesized a triazine ring based imine linked organic polymer that showed the CO_2 uptake of 58.9 weight percentage [21]. The continuous π-conjugation in POPs not only represents its ability to adsorb and separate gas molecules, but also exhibits excellent candidature for the adsorption of hydrocarbons. Ma et al. for the first time reported the selective adsorption of ethylene over ethane by POP introducing π-complexation [5]. POP with envelop of π-electrons hold potent promise in heterogeneous catalysis as catalyst with no metal adds-on and the catalytic bed facilitates the incorporation of metals to act as promising catalyst. A metal coordinated conjugated

microporous polymers (CMPs) exhibited remarkable catalytic activity in the conversion of atmospheric CO_2 gas [22]. Kitagawa in 2007 illustrated the splendid role of amide functionalized porous coordination polymer as catalyst in performing Knoevenagel condensation reaction [23]. The condensation reaction has been performed exploiting the basicity of amide linked metal free POP acting as organocatalyst [24]. Zhou et al. added further dig into the utility of amide functionalized porous network in organic reaction mechanisms [25]. The porous network acts as a cooperative catalyst in deacetalization-Knoevenagel condensation reaction. It is noteworthy to mention that in recent times porous materials have been emerging as an interesting heterogeneous catalyst in various organic transformation reactions. Moreover the extended π-electron clouds in the porous materials provide a platform to represent them as support matrix for transition metals in performing catalytic reactions [26]. The amide functionality in 2D POP with continuous π-conjugation has been exploited as an active center in catalysis [27]. We have recently demonstrated such amide linked materials as organocatalyst in promoting the selective oxidation of benzyl alcohol to the corresponding benzaldehyde and discussed in Chapter 2.

Present study is sought to design and synthesis of a new triazine ring based microporous organic polymer with amide functionality by Schiff-base condensation reaction. The desired polymer (POP-Am2 hereafter) has been employed as catalytic support in Wacker oxidation, the catalytic oxidation of alkenes affording carbonyl compounds. POP-Am2 was found remarkably active as catalyst towards Wacker-type oxidation of α-aryl substituted olefins into uncommon benzaldehyde formation selectively. It is accompanied by C=C double bond cleavage to produce benzaldehyde as major product, a rare outcome in olefin oxidation using organic catalyst supported by experiments and computational study. The reaction was further tested using POP-Am2 in carbon-carbon triple bonds successfully.

4.3 Results and discussion

4.3.1 Synthesis of nitrogen rich triazine based porous polymer

A high nitrogen content porous organic polymer network solid with carboxamide functionality has been synthesized from 2,4,6-tris(4-aminophenyl)triazine (TAPT) and 1,3,5-benzenetricarbonyl trichloride (BzCl) (Scheme 4.1). The triazine ring based building unit TAPT is synthesized from 4-aminobenzonitrile following a reported

procedure. Details are available in experimental section. The POP-Am2 is characterized by FT-IR, PXRD, TGA, BET, TEM, SEM, etc. characterization tools.
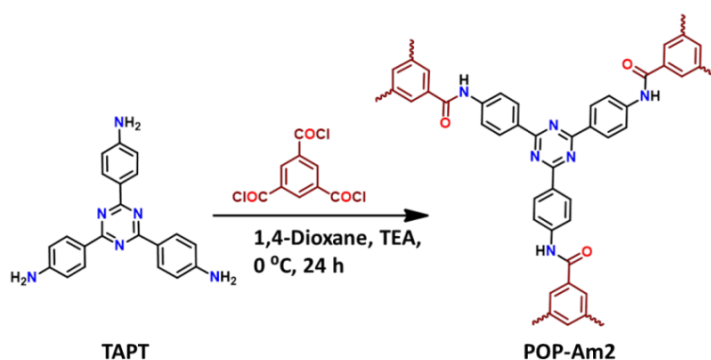
Scheme 4.1 Schematic representation of synthesis of microporous POP-Am2 from TAPT.

4.3.2 Characterization of POP-Am2

Indication over the formation of TAPT from 4-aminobenzonitrile (4ABN) for the synthesis of POP-Am2 was initially detected from FT-IR spectrum (Figure 4.1a). The strong absorption band at 1503 cm^{-1} and 1360 cm^{-1} advocates the successful formation of triazine ring. Also, the strong absorption at 2235 cm^{-1} responsible for C≡N in 4ABN is absent signifying the purity of TAPT .
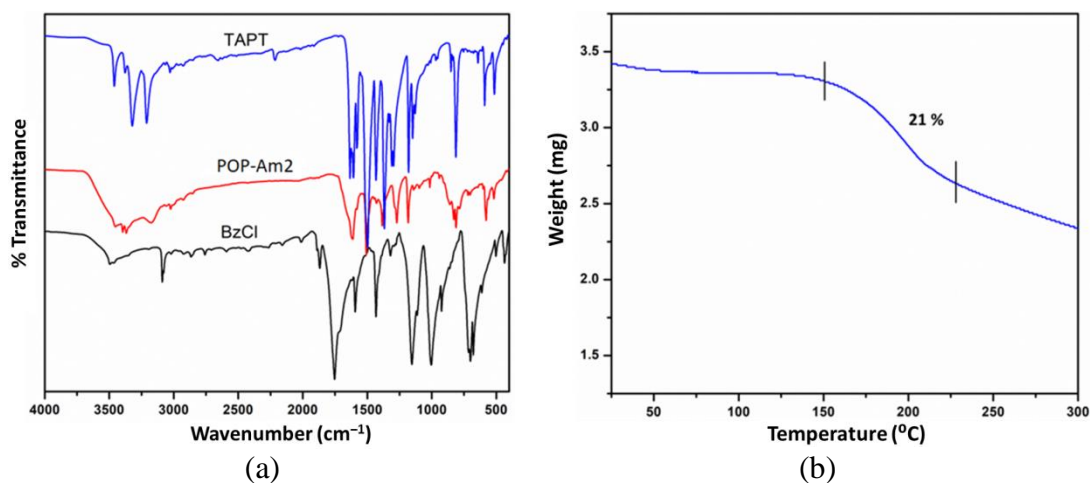

Figure 4.1 (a) FT-IR spectra comparison of POP-Am2 with its building units, (b) TGA plot displaying the stability and inclusion of guest molecules in the pores of POP-Am2.

The formation of TAPT is further confirmed by ^{1}H- and ^{13}C- NMR spectrum. The singlet at 5.88 ppm for six NH$_2$ protons and two doublets at 6.65 and 8.31 ppm (for 12 aromatic protons) in the spectrum firmly assure the formation of TAPT (Figure 4.2a). The ^{13}C

chemical shift of TAPT appears at 113, 123, 130, 153, 170 ppm respectively (Figure 4.2b).
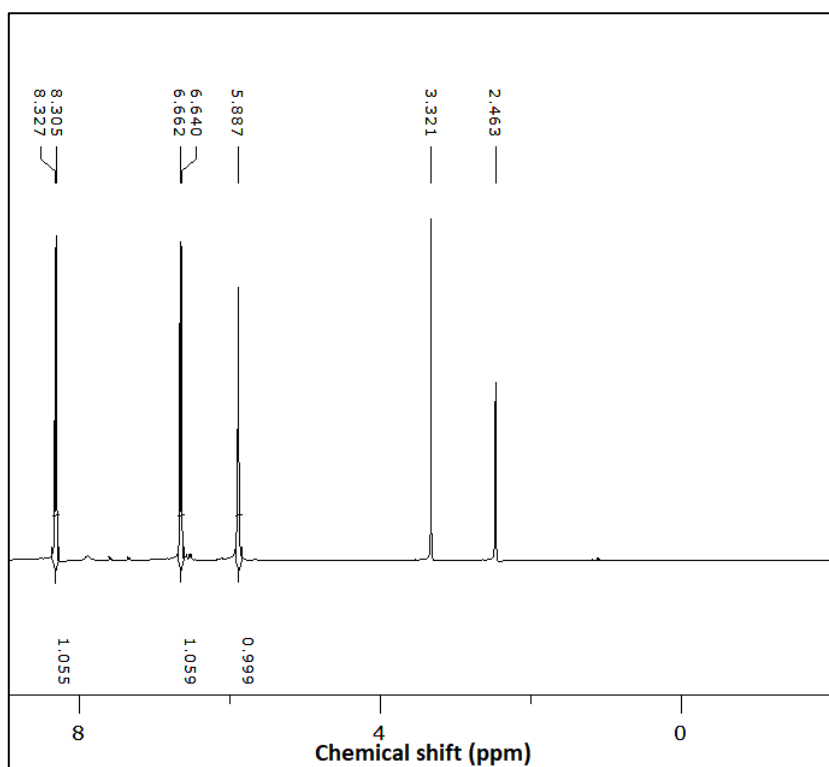
(a)
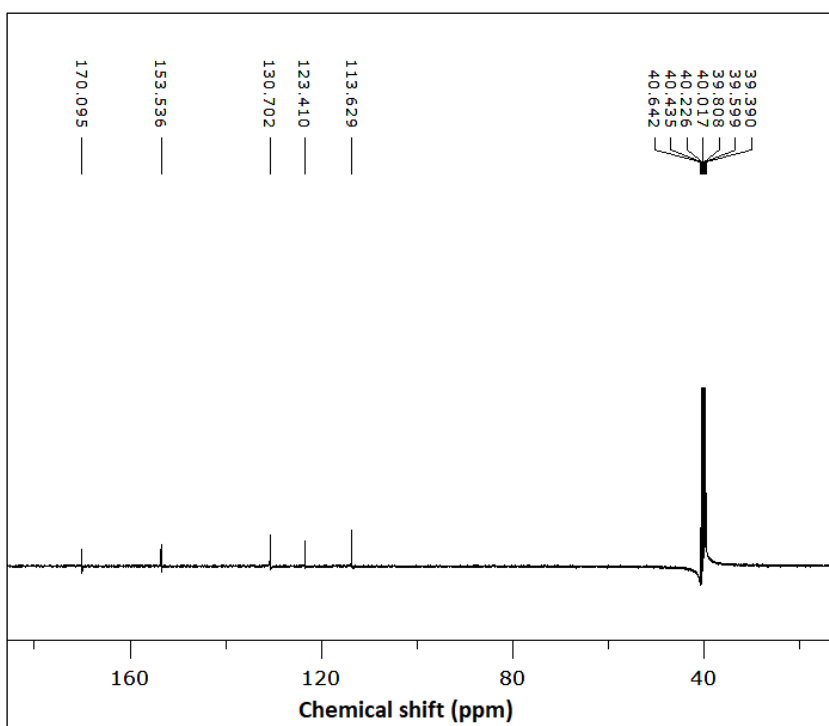
(b)

Figure 4.2 ^{1}H NMR (a) and ^{13}C NMR (b) spectrum of TAPT recorded in DMSO-d_6.

In order to examine the bonding functionality in POP-Am2, FT-IR and solid state NMR (ssNMR) was recorded. The stretching frequency of carbonyl chloride C=O of BzCl at 1753 cm^{-1} vanishes and the frequency responsible for amide C=O advents at 1616 cm^{-1} (Figure 4.1a) indicating the presence of amide C=O functionality and thereby formation of desired amide linked POP-Am2.

The TGA analysis of synthesized POP-Am2 reveals excellent thermal stability up to 300 ºC (Figure 4.1b) with weight loss of about 21 % in the range 150 to 225 ºC. This loss might be due to the trapping of guest molecules in the cavities of the host. The porous polymer was further activated at 200 ºC for 1 h at furnace ensuring it to be guest free host. The guest free POP-Am2 was then subjected for further study.

Information about the trapped guest molecules was gathered by recording the PXRD pattern of as synthesized followed by thermal activation of POP-Am2 materials. The pattern of as synthesized material displays some degrees of freedom attributed by few intense peaks (Figure 4.3a). The intense peaks at 2θ range 10 º to 30 º are responsible for triethylammonium chloride salt and a detail discussion is available in Chapter 3 under results and discussion. Thus, the trapping of HCl by triethylamine (TEA) in the cavities of POP-Am2 could be concluded. The HCl is evolved during the condensation reaction of building units affording the porous polymeric network solid. The PXRD pattern of activated solid (Figure 4.3a) reveals the material amorphous in nature. The broad peak at 2θ ranging from 20 º to 30 º exhibits due to the presence of extended π–clouds of 2D sheet like structure of the network solid.

As POP-Am2 is practically insoluble in common organic solvents the ssNMR analysis could be a handy tool to analyze and verify the chemical environments of carbon centres in the polymeric network. The chemical shift value at 163 ppm indicates the presence of amide carbonyl carbon. Whereas the signal peak at 170 ppm signifies the existence of triazine ring in the framework and peaks at 152, 150, 141, 131, 119 and 118 ppm further attributes to the aromatic carbon peak in POP-Am2. The absence of any extra peak in the spectrum nullifies the presence of unreacted BzCl and TAPT also assures the purity of POP-Am2.

(a)   (b)
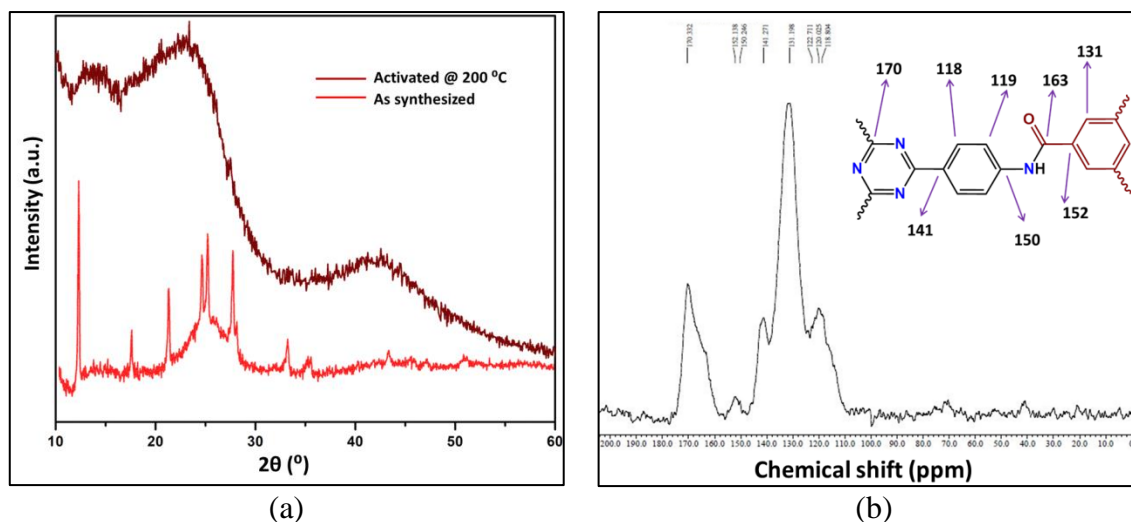
Figure 4.3 (a) PXRD pattern of synthesized POP-Am2 displaying the inclusion of triethylammonium chloride salt in its cavities that releases upon thermal activation signifying amorphous nature. (b) ^{13}C ssNMR spectrum and the chemical environments of POP-Am2.

In order to gather further insight into the porosity and rigidity of POP-Am2 the BET surface area analysis has been carried out. Figure 4.4a displaying volume of N_2 adsorption-desorption isotherm of activated POP-Am2 which assigns type II isotherm. The surface area and pore diameter in POP-Am2 are calculated at 51 m^2/g and of 1.5 nm respectively. The low surface area and small pore size might be attributable to the unordered skeleton structure and blockage of the channels due to interweaving of outgrowth arms during polymerization. The pore size distribution curve for N_2 adsorption is demonstrated in Figure 4.4b.

(a)   (b)
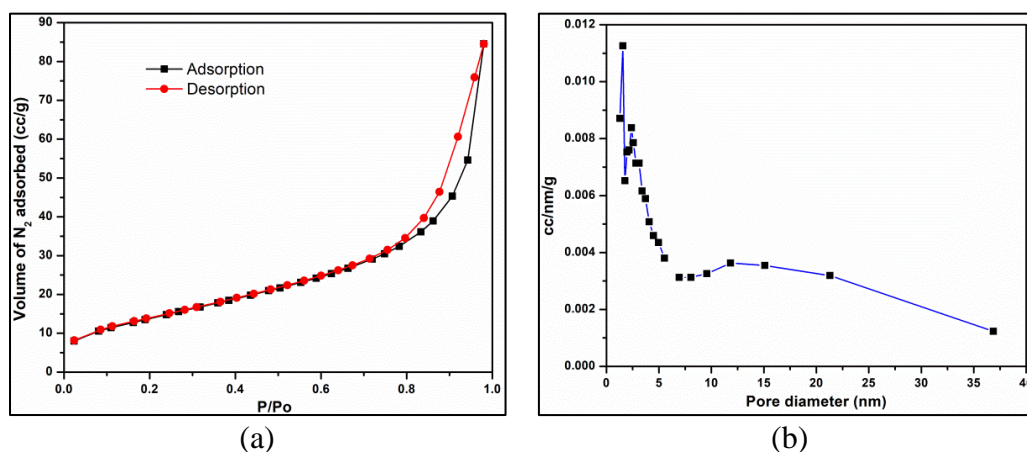
Figure 4.4 Nitrogen adsorption-desorption isotherm (a) and pore size distribution curve (b) of POP-Am2.

(a)   (b)
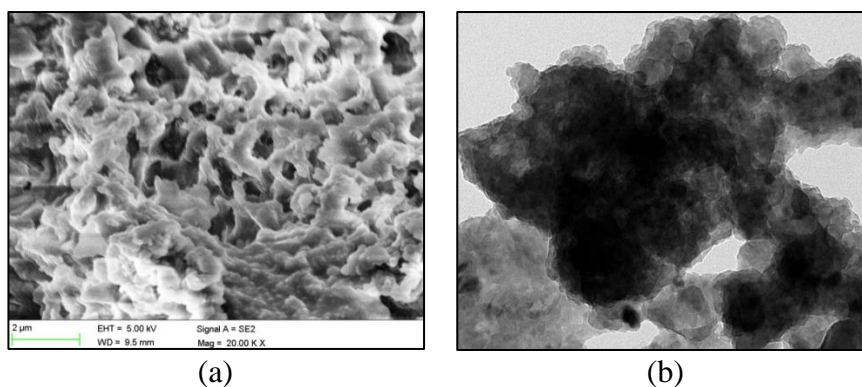
Figure 4.5 FE-SEM (a) and TEM (b) image of POP-Am2.

To understand the surface morphology of POP-Am2, microscopic analysis has been performed. The FE-SEM image (Figure 4.5a) of the solid network reveals regular morphology of POP-Am2 with clear visibility of porosity. In addition, information provided by TEM image (Figure 4.5b) attributes the stacked 2D sheet like behavior with extended network with microporous structure. Such sheet like morphologies has also been exhibited by many reported 2D covalent organic frameworks available in the literature.

4.3.3 Oxidation of α-aryl substituted olefins

Owing to the presence of basic functionality and other heterogeneous atom (N and O) in the pore wall and surfaces of the network solid, POP-Am2 is expected to show efficient affinity towards gas uptake. Lewis acid-base and dipole-quadruple interactions propensity provokes POP-Am2 to capture acidic gas like CO_2. It has also been established that the π-electrons rich porous polymers can serve as an excellent bed for catalysis. Stimulated by the remarkable activities of amide polymeric network in catalysis, the characterized POP-Am2 having dual catalytic sites (amide –CONH– and N of the triazine ring with free lone pair) with extended π-cloud was further considered to investigate as organocatalyst in the oxidation of α-aryl substituted olefins. Initially, the catalytic activity of POP-Am2 is tested for the oxidation of styrene (Scheme 4.2) with *tert*-butyl hydroperoxide (TBHP). Under optimized reaction conditions at 8 h with 10 % (w/w) POP-Am2 with respect to styrene were allowed to react. It produces benzaldehyde in major selectivity accomplished by the C=C bond cleavage along with other products viz. styrene oxide and 2-phenyl ethanal in minor quantity.
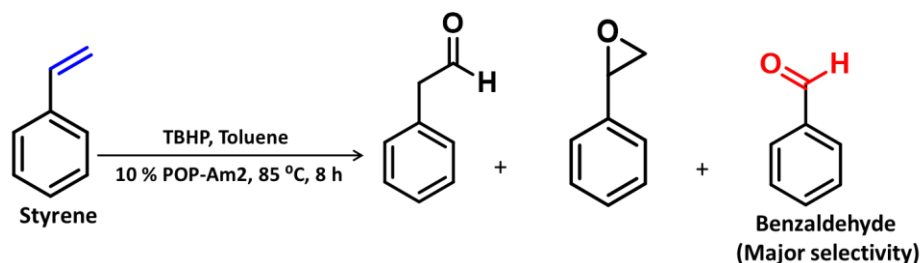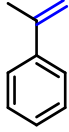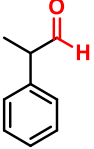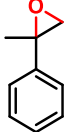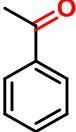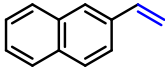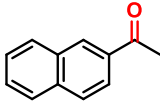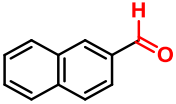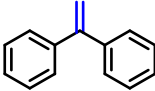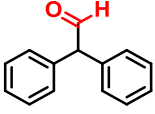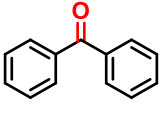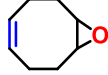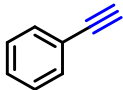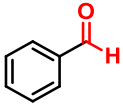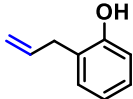
Scheme 4.2 Schematic representation of styrene oxidation using POP-Am2 afforded benzaldehyde in major selectivity by C=C bond cleavage. Epoxide and terminal aldehyde are other by-products in minor selectivity.

The success in oxidation of styrene accompanying C=C bond cleavage prompted to test the catalytic influence of POP-Am2 in other substituted styrenes (Table 4.1). Interestingly each substrate resulted in cleavage of C=C bond yielding the corresponding benzaldehydes in major selectivity along with other minor by-products (Table 4.1) as revealed by GC-MS analysis. In fact, even C≡C bond in phenyl acetylene was tested. Surprisingly the triple bond has also cleaved resulting same results of benzaldehyde formation but relatively lesser yield percentage. Amongst the varied substrates maximum conversion of 87 % was observed in case of 2-vinylnaphthalene (Entry 7, Table 4.1) and the highest selectivity is 92 % for benzaldehyde experienced in 4-methoxystyrene (Entry 2, Table 4.1). Notably, during the process of oxidation the curiosity towards control oxidation of styrene yielding corresponding oxide increases.

Table 4.1 POP-Am2 as promoter in the oxidation of styrene derivatives affording benzaldehydes

Sl No.	R	Conversion %	Product yield %			
			I	II	III	IV
1	H	60	4	-	36	60
2	OMe	74	-	8	-	92
3	Cl	49	-	3	38	59
4	Me	21	-	-	-	21

5	NO$_2$	29	-	-	-	29

Reactant	Conversion %	Product Yield %		
6	59	10	12	78
7	87		20	80
8	12		34	66
9	10		10	
10	27		27	
11	ND*		ND	
12	ND		ND	

*ND: Not detected any product formation in GC-MS analysis.

Under the optimum conditions no conversion of styrene in presence of TBHP and absence of POP-Am2 was observed. This means the POP-Am2 has definite role in influencing the reaction pathway. Furthermore the oxidation was not facilitated to considerable conversion while H$_2$O$_2$ was used instead of TBHP (Scheme 4.3) may be due to weaker oxidizing reagent. Moreover, H$_2$O$_2$ is not easily miscible to non-polar solvents such as toluene thereby present investigation is continued with TBHP.

$$H_2O_2, \text{ Toluene}$$
$$\xrightarrow{\hspace{2cm}} \text{No reaction}$$
$$10\% \text{ POP-Am2, 85 °C, 8 h}$$
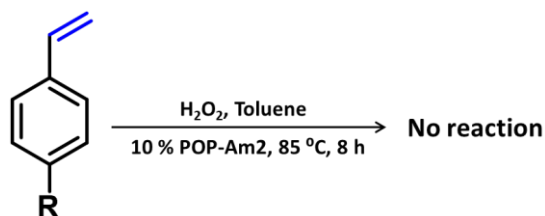
Scheme 4.3 Catalytic oxidation of styrene derivatives does not proceed with H_2O_2 as oxidant in lieu of TBHP.

Examples with peroxide in olefin oxidation includes the formation of metal hydroperoxide intermediates involving peroxide as anion yielding methyl ketone or acetaldehyde in general. The analogous pathway with basic porous polymer, POP-Am2 was expected to give methyl ketone or terminal aldehyde, i.e. acetaldehyde by following Markovnikov's and/or *anti*-Markovnikov's rule. But, in present system the cleavage of C=C bond was observed in all furnishing benzaldehyde as major product and other by-products (epoxide and methyl ketone) in lesser quantity. Eventually, the well-established general mechanistic pathway in olefins oxidation is ruled out and forced to ponder about the plausible route for product formation.

4.3.4 Catalyst reusability test

In catalytic reactions, the efficient reusability of a stable catalyst is important from industrial application perspective. The POP-Am2 experience good reusability in the efficient oxidation of styrene up to 4th cycle with good conversion rate (Figure 4.6a) accompanied by the cleavage of C=C double bond of terminal alkenes.

Between each cycle the catalyst was removed from reaction mixture by centrifugation, washed with acetone and methanol ensuring it to be freed from reactants and products. Dried material and thermally activated before being employed for the subsequent cycles. The conversion % of styrene at each cycle remains almost constant up to third cycle. Whereas at fourth cycle the conversion % decreases. It probably due to the blocking of active catalytic sites in POP-Am2 by CO_2 and H_2 that evolves during the reaction. PXRD patterns of reused material (Figure 4.6b) renders the intact structural integrity of POP-Am2 even after 4th cycle exposing its potent as heterogeneous catalyst.

(a)

(b)
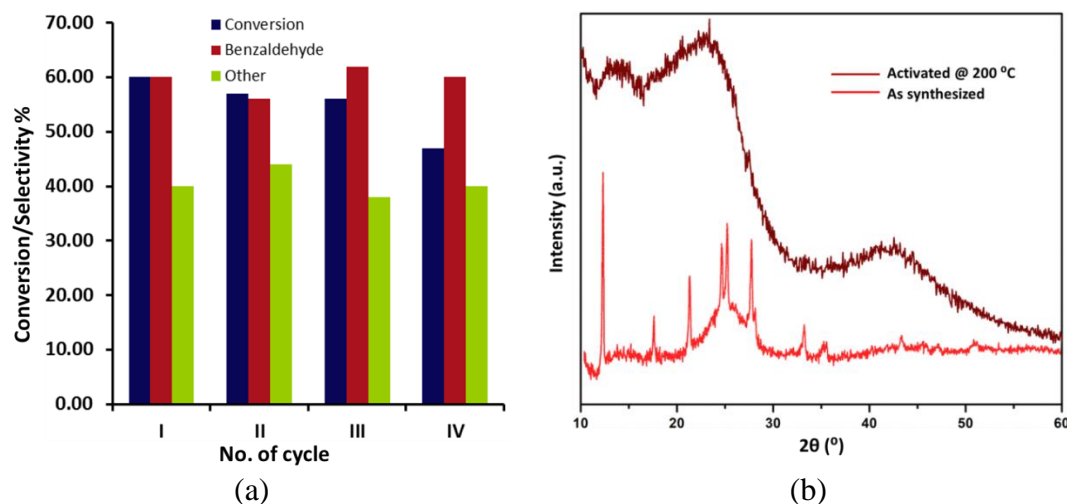
Figure 4.6 (a) Catalytic reusability test of POP-Am2 in oxidation of styrene. (b) PXRD pattern of reused POP-Am2 recorded after 4th cycle and compared to its initial pattern reveals intact structural integrity of POP-Am2 even after catalytic pathways.

4.3.5 Reaction mechanism study

Investigating the structural integrity and functionality in POP-Am2 it was speculated that the reaction could be initiated by the generation of free radicals during the progress of reactions. The carboxamide functionality acts as an active site in generation of radical intermediates from hydroperoxide as discussed in chapter 2. Also, the electron rich π-cloud in POP-Am2 representing as hydrogen bonding receptor site facilitates the radical formation and is explained later. The free radical mechanism in the C=C double bond cleavage of substituted enamines giving the ketonic product has been illustrated [28]. In order to ensure if the reaction mechanism proceeds through radical formation, oxidation of styrene under identical conditions as mentioned in Table 4.1 was performed in presence of TEMPO, a free radical scavenger. As expected the oxidation freezes evidencing the free radical mechanistic pathway for benzaldehyde formation.
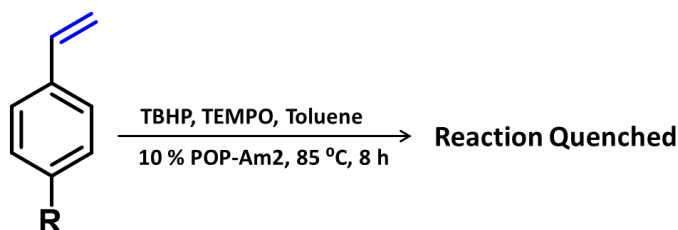
Scheme 4.4 Oxidation of substituted styrene freezes while performing the reaction in presence of a free radical scavenger (TEMPO) evidencing the formation of free radicals during the reaction process.

100
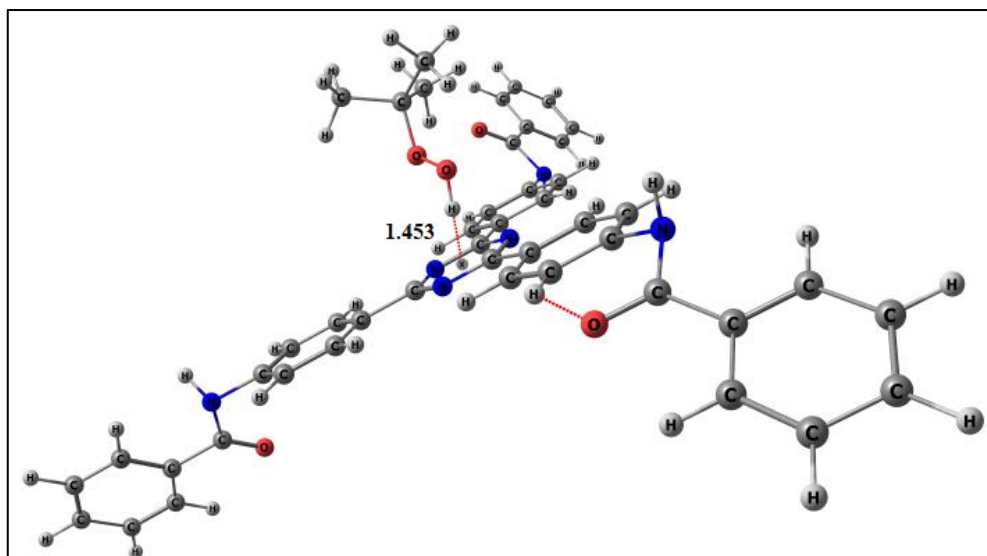
Figure 4.7 Optimized geometry of the trimeric unit in POP-Am2 and the incoming oxidant, TBHP displaying the H-bond interaction with π-cloud of the catalyst.

To support the experimental findings, DFT computational studies have been performed considering the trimeric unit of the catalyst, POP-Am2. The optimized geometry of the complex (bearing the trimer and incoming molecule TBHP, Figure 4.7) shows that they are connected by weak O–H···π non-covalent interaction via the H-atom of incoming molecule and π-cloud of the central ring of the trimer. To further ascertain this interaction, quantum theory of atoms in molecules (QTAIM) analysis (Figure 4.8a) has been carried out [29]. The formation of a bond path as well as its associated bond critical point between the H atom of incoming molecule and π-cloud of the central ring clearly establishes the formation of such interaction. Non-covalent interaction index (NCI) calculation [30] also reveals the formation of attractive zone between them (Figure 4.8b).
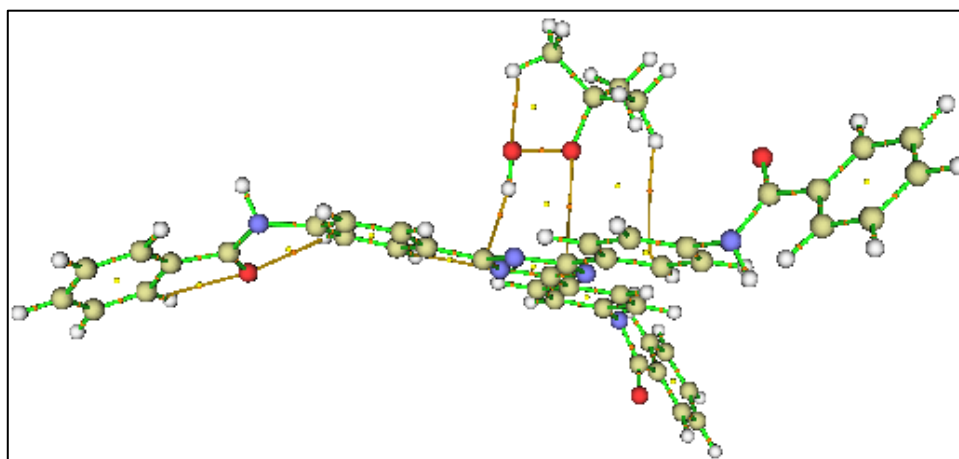
(a)
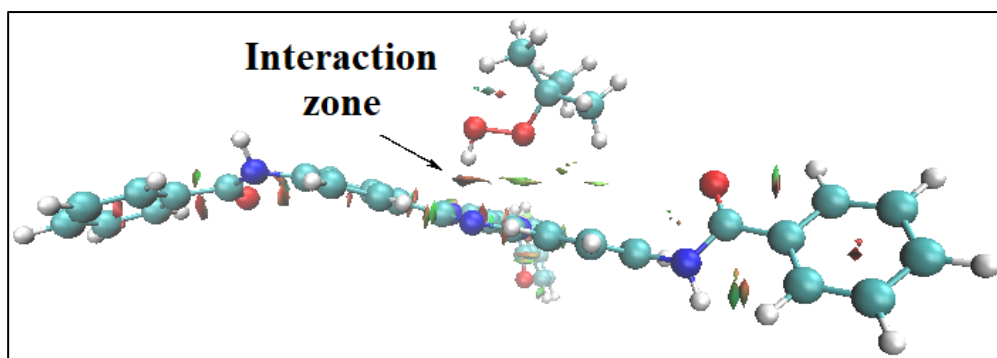
(b)

Figure 4.8 QTAIM analysis attributing the weak interaction between H-atom of TBHP and π-cloud of the central ring of the trimer (a) and NCI calculation revealing the interaction zone between TBHP and the π-cloud of the catalyst (b).

To understand better, the interaction energy is calculated using symmetry adapted perturbation (SAPT) analysis [29]. It was found to be 5.3 kcal/mol, which were further decomposed into electrostatic, dispersion, induction and exchange components (Table 4.2).

Table 4.2 Energies calculated for various interactions associated with TBHP and the catalyst surface.

Electrostatics (kcal/mol)	Induction (kcal/mol)	Dispersion (kcal/mol)	Exchange (kcal/mol)	Total (kcal/mol)
-7.43	-0.88	-2.09	5.10	-5.30

Amongst these four energy components, the first three are attractive while the last one is repulsive. It is evident from the table that electrostatic is the most dominant contributor towards the interaction energy. Whereas, lower value of dispersion indicates that the free rotation of incoming molecule on the surface of the polymer is hindered. The O–O bond length in the optimized geometry of the polymer bound molecule is 1.52Å compared to 1.34Å in the free $(CH_3)_3COOH$ molecule. This indicates that the cleavage of O–O bond to generate OH and $(CH_3)_3CO$ radicals will be energetically favourable.

The energies of generated active radicals are computed and shown in Figure 4.9. Generation of the OH and O^tBu free radicals via interaction with the trimer involves an energy barrier of 56.4 kcal/mol. In the transition state (TS), the O–O bond elongated up to 1.92Å compared to the O–O bond length (1.34Å) in HOO^tBu molecule. This

elongation of O–O bond length in the transition state is an indication towards the homolytic cleavage of O–O bond resulting in the formation of radicals. Subsequent release of the radicals is found to be exergonic by 19.9 kcal/mol. These OH and O^tBu radicals then takes part in the oxidative conversion of α-aryl substituted olefins via C=C bond cleavage.
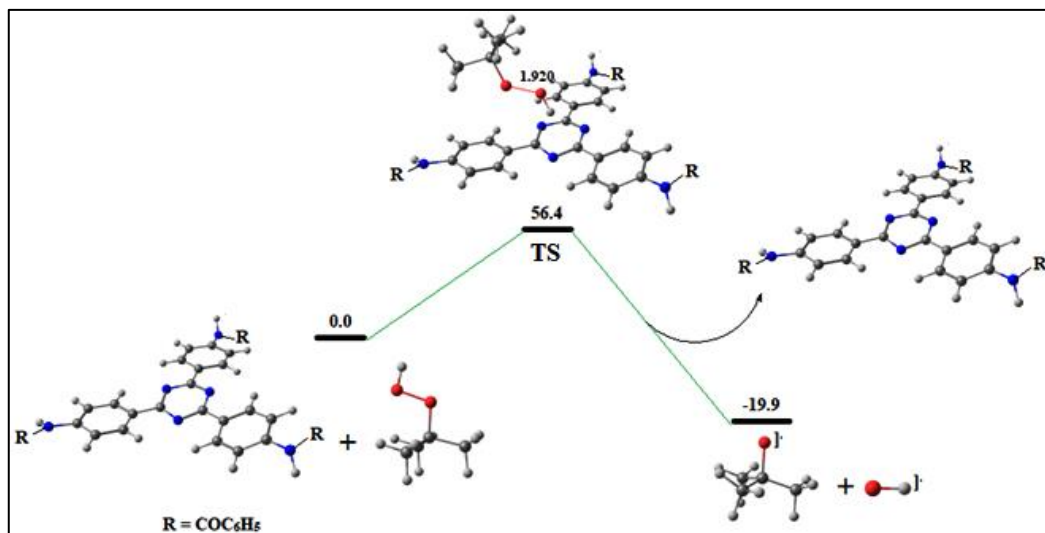
Figure 4.9 Generation of the free radicals mediated by the trimer unit of POP-Am2.

Theoretical conversion of styrene to the oxidized products is shown in Figure 4.10. The attack of OH radical to styrene generating the intermediate (Int-1) is calculated to be exergonic by 37.0 kcal/mol. Int-1 is then attacked by O^tBu radical to generate epoxide intermediate (Int-2) and subsequent release of ^tBuOH takes place. This step is also found to be exergonic by 38.9 kcal/mol. Int-2 is further attacked by ^tBuOOH to generate the intermediate, Int-3, which is also found to exergonic by 16.1 kcal/mol. Finally, Int-3 rearranges to generate the products Prod-1 and Prod-2 with subsequent release of ^tBuOH molecule. Like other steps, this too is calculated to be exergonic by 46.9 kcal/mol. Thus, the overall energetic suggests that all the steps are exergonic and should proceed rapidly just like other free radical mechanisms.

From the experimental evidences and the computational study it is confirmed that the oxidation of α-aryl substituted olefins proceeds through free radical pathway. At the very beginning TBHP moiety gets attached to the catalyst surface via hydrogen bonding (O–H···O=$C_{catalyst}$ or O–H···$N_{catalyst}$) and directional O–H···π interaction with catalyst surface. Thereby, the peroxide O–O bonding gets weakened, generating the hydroxyl and *tert-*

butoxy radicals as shown in Figure 4.9. The generated radicals get stabilized at the catalyst surface via directional O–H⋯π interaction as the catalyst with N heteroatom in structural architecture is rich in π-cloud propagated by amide functionality. The OH radical once sense the presence of nearby styrene which is being stabilized at catalyst surface via π⋯π and/or C–H⋯π interaction perhaps initially attacks the terminal carbon of C=C bond in styrene generating benzylic radical substituent (Int-1, Figure 4.10). Thus generated radical species that remains stabilized due to delocalization with benzene ring provides kick towards oxidation reaction process. Subsequently, *tert*-butoxy radical detaches the hydroxyl proton from benzylic radical substituent, get converts itself to *tert*-butanol and styrene oxide evokes simultaneously (Int-2, Figure 4.10). Consequently, ring opening of styrene oxide is accomplished by the excess of TBHP in reaction mixture as shown in Figure 4.10 eventually leading to the formation of desired benzaldehyde and formaldehyde. The formaldehyde upon oxidation followed by heating evolves CO_2 and H_2 gas. Possibly, the liberated gases are adsorbed by POP-Am2 since the nitrogen rich porous network solids are prone to behave so. And, the benzaldehyde is stabilized strongly over the catalyst surface thereby precluding the possibility of over oxidation.
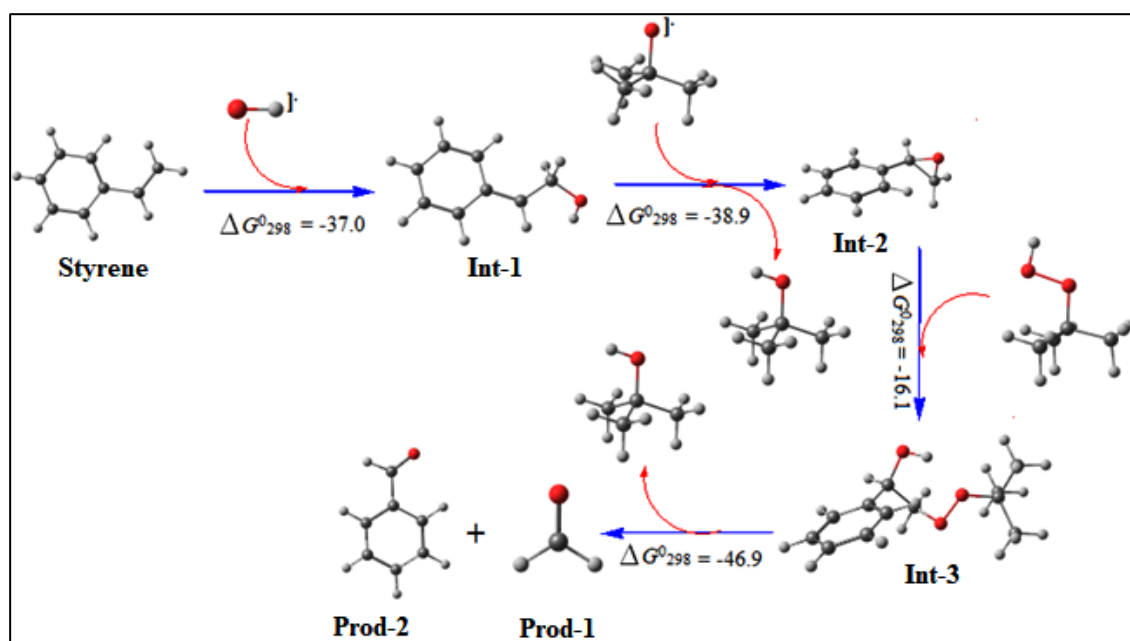
Figure 4.10 Gibbs free energy changes during the radical initiated product formation during styrene oxidation to aldehyde stimulated by POP-Am2.

4.4 Summary

A new nitrogen rich microporous organic polymer with amide functionality has been synthesized and characterized using spectroscopic, microscopic, X-ray diffraction and surface area analyzer techniques. The polymer i.e. POP-Am2 exhibits remarkable applications as potent organocatalyst in the cleavage of C=C bond of substituted styrene and C≡C bond of phenyl acetylene affording benzaldehyde in major selectivity. Thus, the oxidation of alkenes with high selectivity in benzaldehyde formation but not with formation of methyl ketone and/or substituted acetaldehyde catalyzed by precious metal (Pd, Pt, Ru, Rh, Au, etc.) complexes following Markovnikov's and *anti*-Markovnikov's rule is exciting and reasoned with evidences. This paves the way towards a new avenue of applications of POP as metal free catalyst in performing organic transformation reactions.

4.5 Experimental Section

4.5.1 Materials

All the chemicals employed are brought from commercial sources and were used as such without further purification until otherwise mentioned. 4-Aminobenzonitrile (4ABN), triflic acid, styrene derivatives and 1,3,5-benzenetricarbonyl trichloride (BzCl) were purchased from Alfa Aesar. All solvents of HPLC grade, triethylamine (TEA), TLC silica gel F254 250 μm precoated-plates and 1,4-dioxane used in the experiments were procured from Merck.

4.5.2 Synthesis of 2,4,6-tris-(4-aminophenyl)triazine (TAPT)

The triazine building unit is prepared using 4-aminobenzonirile (4ABN) by following reported procedure [31]. Added dropwise 2 mL triflic acid to 720 mg of 4ABN with continuous stirring in an ice cold nitrogenous environment and allowed it to continue for another 24 h. Poured 10 ml distilled water to the reaction mixture followed by dropwise addition of 2M NaOH at room temperature until bright yellow colour precipitate appears. Meanwhile the pH of the solution is monitored till it reaches at 7. The light yellow precipitate was filtered, washed with distilled water, dried and characterized with NMR spectroscopy.

^{1}H NMR (DMSO-D$_6$, 400 MHz): δ (ppm) = 5.88 (*s*, 6H), 6.65(*d*, 6H, *J* = 8.4 Hz), 8.31 (*d*, 6H, *J*=8.4 Hz); ^{13}C NMR (DMSO-D$_6$, 400 MHz): δ (ppm) = 113, 123, 130, 153, 170.

4.5.3 Synthesis of amide linked triazine ring based organic polymer (POP-Am2)

Dissolved 720 mg (1mmol) of TAPT in 25 mL of dry 1,4-dioxane and kept in an ice cold water bath adding 2 mL of triethylamine (TEA). Added to it the solution of 265 mg (1 mmol) of 1,3,5-benzenetricarbonyl trichloride (BzCl) in dry 1,4-dioxane (10 mL) slowly over a period of 2 h in nitrogenous environment and left with continuous stirring for 12 hours. Special care should be taken during the reaction as the corrosive HCl gas liberates during the condensation. The desired precipitate of POP-Am2 is then filtered and washed with acetone. The solubility of all other unreacted particle and undesired product in acetone except the desired one allow us to get a pure expected framework material by washing it with acetone. It is then dried in desiccator so as to remove the captured solvent molecule and is further characterized.

4.5.4 Characterization/Instrumentation

4.5.4.1 FT-IR spectroscopy

FT-IR spectra of the building units and the desired polymeric solid POP-Am2 were recorded in the frequency range of 400–4000 cm^{-1} in PerkinElmer spectrophotometer. Details of the experimental procedure in recording the spectrum is same as discussed in Chapter 2.

4.5.4.2 Thermogravimetric (TGA) analysis

The thermal stability of POP-Am2 and the information about inclusion of any guest molecules or impurities is drawn from TGA analysis. Details about the experimental techniques and the instrumentation is same as furnished in Chapter 2.

4.5.4.3 Powder X-ray diffraction (PXRD) analysis

Detail about sample preparation technique and the instrument is described in Chapter 2 and same procedure is followed.

4.5.4.4 NMR spectroscopy

The chemical environment in TAPT has been studied by recording the ^{1}H and ^{13}C NMR spectra in deuterated DMSO-d_6 in Jeol 400 MHz spectrophotometer. The chemical environment of polymer POP-Am2 is studied recording solid state NMR (ssNMR) spectrum. Detail about the procedure and instrumentation is explained in Chapter 2.

4.5.4.5 BET surface area analysis

The surface area, type of adsorption isotherm and porosity associated in POP-Am2 is collected from Brunauer-Emmett-Teller (BET) surface area analyzer. A detail about the procedure and instrument is same as described in Chapter 2.

4.5.4.6 Electron microscopy

The detail procedure about sample preparation and instruments in recording the microscopic image is described in Chapter 2. Identical method is followed herein.

4.5.4.7 Gas chromatography-mass spectrometry (GC-MS) technique

GC-MS technique has been considered in order to investigate and characterize the reaction mixture. Detail about the work-up procedure and the sample preparation process is described in Chapter 2 and is followed here.

4.5.4.8 Computational Details

Structures optimization were performed in B3LYPD3BJ level of theory [32] by means of 6-311++G** basis set. Correction of interaction energies in the process for BSSE (basis set superposition error) has been performed by the "Counterpoise = N" choice employing the Boys and Bernardi's counterpoise method [33]. All calculations were accomplished using GAUSSIAN16 suite of program [34].

4.5.4.9 Procedure for catalytic reaction

Added 100 µL of styrene to 1 mL of toluene solution taken in a dry schlenk tube and to this mixture placed *tert*-butylhydroperoxide, TBHP (styrene:TBHP = 1:2 molar ratio) and 10 weight % POP-Am2 with respect to styrene. The whole mixture was heated at 85 ⁰C for 8 h. After completion of reaction, the progress was monitored by TLC measurement and product formation was analyzed by GC-MS analyzer.

4.6 References

[1]   Strukul, G., Ros, R. and Michelin, R. A. Preparation and Oxygen-Transfer Properties of Novel Palladium(II) and Platinum(II) Hydroperoxo and Alkylperoxo Complexes. *Inorganic Chemistry*, 21(2):495-500, 1982.

[2] Mimoun, H., Perez Machirant, M. M. and Seree de Roch, I. Activation of Molecular Oxygen: Rhodium-Catalyzed Oxidation of Olefins. *Journal of the American Chemical Society*, 100(17):5437-5444, 1978.

[3] Roussel, M. and Mimoun, H. Palladium-Catalyzed Oxidation of Terminal Olefins to Methyl Ketones by Hydrogen Peroxide. *The Journal of Organic Chemistry*, 45(26):5387-5390, 1980.

[4] Walker, K. L., Dornan, L. M., Zare, R. N., Waymouth, R. M. and Muldoon, M. J. Mechanism of Catalytic Oxidation of Styrenes with Hydrogen Peroxide in the Presence of Cationic Palladium (II) Complexes. Journal of the American Chemical Society, 139(36):12495-12503, 2017.

[5] Michel, B. W., Steffens, L. D. and Sigman, M. S. On the Mechanism of the Palladium- Catalyzed *tert*-Butylhydroperoxide-Mediated Wacker-Type Oxidation of Alkenes Using Quinoline-2-Oxazoline Ligands. *Journal of the American Chemical Society*, 133(21):8317-8325, 2011.

[6] Kim, K. E., Li, J., Grubbs, R. H. and Stoltz, B. M. Catalytic Anti-Markovnikov Transformations of Hindered Terminal Alkenes Enabled by Aldehyde-Selective Wacker-Type Oxidation. *Journal of the American Chemical Society*, 138(40):13179-13182, 2016.

[7] Ning, X. S., Wang, M. M., Yao, C. Z., Chen, X. M. and Kang, Y. B. *tert*-Butyl Nitrite: Organic Redox Cocatalyst for Aerobic Aldehyde-Selective Wacker–Tsuji Oxidation. *Organic Letters*, 18(11):2700-2703, 2016.

[8] Wickens, Z. K., Skakuj, K., Morandi, B. and Grubbs, R. H. Catalyst-Controlled Wacker-Type Oxidation: Facile Access to Functionalized Aldehydes. *Journal of the American Chemical Society*, 136(3):890-893, 2014.

[9] Jiang, Y. Y., Zhang, Q., Yu, H. Z. and Fu, Y. Mechanism of Aldehyde-Selective Wacker-Type Oxidation of Unbiased Alkenes with a Nitrite Co-Catalyst. *ACS Catalysis*, 5(3):1414-1423, 2015.

[10] Michel, B. W., Steffens, L. D. and Sigman, M. S. On the Mechanism of the Palladium-Catalyzed *tert*-Butylhydroperoxide-Mediated Wacker-Type Oxidation of Alkenes Using Quinoline-2-Oxazoline Ligands. *Journal of the American Chemical Society*, 133(21):8317-8325, 2011.

[11] Wickens, Z. K., Guzmán, P. E. and Grubbs, R. H. Aerobic Palladium-Catalyzed Dioxygenation of Alkenes Enabled by Catalytic Nitrite. *Angewandte Chemie International Edition*, 54(1): 236-240, 2015.

[12] Muzart, J. Aldehydes from Pd-Catalysed Oxidation of Terminal Olefins. *Tetrahedron*, 63(32):7505-7521, 2007.

[13] Parshamoni, S., Telangae, J., Sanda, S. and Konar, S. A Copper-Based Metal–Organic Framework Acts as a Bifunctional Catalyst for the Homocoupling of Arylboronic Acids and Epoxidation of Olefins. *Chemistry–An Asian Journal*, 11(4):540-547, 2016.

[14] Mu, M., Wang, Y., Qin, Y., Yan, X., Li, Y. and Chen, L. Two-Dimensional Imine-Linked Covalent Organic Frameworks as a Platform for Selective Oxidation of Olefins. *ACS Applied Materials & Interfaces*, 9(27):22856-22863, 2017.

[15] Feng, B., Hou, Z., Wang, X., Hu, Y., Li, H. and Qiao, Y. Selective aerobic oxidation of styrene to benzaldehyde catalyzed by water-soluble palladium (II) complex in water. *Green Chemistry*, 11(9):1446-1452, 2009.

[16] Duarte, T. A., Carvalho, A. P. and Martins, L. M., Ultra-fast and selective oxidation of styrene to benzaldehyde catalyzed by a C-scorpionate Cu (II) complex. *Catalysis Science & Technology*, 8(9):2285-2288, 2018.

[17] Mu, M., Wang, Y., Qin, Y., Yan, X., Li, Y. and Chen, L. Two-Dimensional Imine-Linked Covalent Organic Frameworks as a Platform for Selective Oxidation of Olefins. *ACS Applied Materials & Interfaces*, 9(27):22856-22863, 2017.

[18] Kaur, P., Hupp, J. T. and Nguyen, S. T. Porous Organic Polymers in Catalysis: Opportunities and Challenges. *ACS Catalysis*, 1(7):819-835, 2011.

[19] Jiang, X., Wang, P. and Zhao, J. 2D covalent triazine framework: a new class of organic photocatalyst for water splitting. *Journal of Materials Chemistry A*, 3(15):7750-7758, 2015.

[20] Zhang, Y. and Riduan, S. N. Functional porous organic polymers for heterogeneous catalysis. *Chemical Society Reviews*, 41(6):2083-2094, 2012.

[21] Gomes, R., Bhanja, P. and Bhaumik, A. A triazine-based covalent organic polymer for efficient CO_2 adsorption. *Chemical Communications*, 51(49):10050-10053, 2015.

[22] Xie, Y., Wang, T. T., Liu, X. H., Zou, K. and Deng, W. Q. Capture and conversion of CO_2 at ambient conditions by a conjugated microporous polymer. *Nature Communications*, 4:1960, 2013.

[23] Hasegawa, S., Horike, S., Matsuda, R., Furukawa, S., Mochizuki, K., Kinoshita, Y. and Kitagawa, S. Three-Dimensional Porous Coordination Polymer Functionalized with Amide Groups Based on Tridentate Ligand: Selective Sorption and Catalysis. *Journal of the American Chemical Society*, 129(9):2607-2614, 2007.

[24] Suresh, V. M., Bonakala, S., Atreya, H. S., Balasubramanian, S. and Maji, T. K. Amide Functionalized Microporous Organic Polymer (Am-MOP) for Selective CO_2 Sorption and Catalysis. *ACS Applied Materials & Interfaces*, 6(7):4630-4637, 2014.

[25] Park, J., Li, J. R., Chen, Y. P., Yu, J., Yakovenko, A. A., Wang, Z. U., Sun, L. B., Balbuena, P. B. and Zhou, H. C. A versatile metal–organic framework for carbon dioxide capture and cooperative catalysis. *Chemical Communications*, 48(80):9995-9997, 2012.

[26] Mondal, J., Trinh, Q. T., Jana, A., Ng, W. K. H., Borah, P., Hirao, H. and Zhao, Y. Size-Dependent Catalytic Activity of Palladium Nanoparticles Fabricated in Porous Organic Polymers for Alkene Hydrogenation at Room Temperature. *ACS Applied Materials & Interfaces*, 8(24):15307-15319, 2016.

[27] Khatioda, R., Talukdar, D., Saikia, B., Bania, K. K. and Sarma, B. Constructing two dimensional amide porous polymer to promote selective oxidation reactions. *Catalysis Science & Technology*, 7(14):3143-3150, 2017.

[28] Adib, M., Pashazadeh, R., Gohari, S. J. A. and Shahsavari, F., Metal-Free Oxidative C=C Bond Cleavage of Electron-Deficient Enamines Promoted by *tert*-Butyl Hydroperoxide. *Synlett*, 28(12):1481-1485, 2017.

[29] Kashyap, C., Ullah, S. S., Mazumder, L. J. and Guha, A. K. Non-covalent Interaction in Benzene and Substituted Benzene: A Theoretical Study. *Computational and Theoretical Chemistry*, 1130:134-139, 2018.

[30] Contreras-García, J., Johnson, E. R., Keinan, S., Chaudret, R., Piquemal, J. P., Beratan, D. N. and Yang, W. NCIPLOT: A Program for Plotting Noncovalent Interaction Regions. *Journal of Chemical Theory and Computation*, 7(3):625-632, 2011.

[31] Gomes, R., Bhanja, P. and Bhaumik, A. A triazine-based covalent organic polymer for efficient CO_2 adsorption. *Chemical Communications*, 51(49):10050-10053, 2015.

[32] Johnson, E. R. and Becke, A. D. A post-Hartree-Fock model of intermolecular interactions: Inclusion of higher-order corrections. *The Journal of Chemical Physics*, 124(17):174104, 2006.

[33] Boys, S. F. and Bernardi, F. D. The calculation of small molecular interactions by the differences of separate total energies. Some procedures with reduced errors. *Molecular Physics*, 19(4):553-566, 1970.

[34] Frisch, M. J., Trucks, G. W., Schlegel, H. B., Scuseria, G. E., Robb, M. A., Cheeseman, J. R., Scalmani, G., Barone, V., Petersson, G. A., Nakatsuji, H. and Li, X., Gaussian 16 Revision A.03, Gaussian Inc., *Wallingford CT*, 2016